



**POLITECNICO**  
MILANO 1863

**[RE.PUBLIC@POLIMI](#)**

Research Publications at Politecnico di Milano

## Post-Print

This is the accepted version of:

G.L. Ghiringhelli, M. Terraneo  
*Analytically Driven Experimental Characterisation of Damping in Viscoelastic Materials*  
Aerospace Science and Technology, Vol. 40, 2015, p. 75-85  
doi:10.1016/j.ast.2014.10.011

The final publication is available at <https://doi.org/10.1016/j.ast.2014.10.011>

Access to the published version may require subscription.

**When citing this work, cite the original published paper.**

© 2015. This manuscript version is made available under the CC-BY-NC-ND 4.0 license  
<http://creativecommons.org/licenses/by-nc-nd/4.0/>

Permanent link to this version

<http://hdl.handle.net/11311/868398>

# Analytically Driven Experimental Characterisation of Damping in Viscoelastic Materials

Gian Luca Ghiringhelli

Politecnico di Milano, Department of Aerospace Science and Technology, Milano, Italy

Mauro Terraneo

VICOTER, Calolziocorte (CO), Italy

## ABSTRACT

The damping assessment of highly dissipative materials is a challenging task that has been addressed by several researchers; in particular Oberst defined a standard method to address the issue. Experimental tests are often hindered by the poor mechanical properties of most viscoelastic materials; these characteristics make experimental activities using pure viscoelastic specimens prone to nonlinear phenomena. In this paper, a mixed predictive/experimental methodology is developed to determine the frequency behaviour of the complex modulus of such materials. The loss factor of hybrid sandwich specimens, composed of two aluminium layers separated by the damping material, is determined by experimental modal identification. Finite element models and a reversed application of the modal strain energy technique are then used to recover the searched storage modulus and loss factor curves of rubber.

In particular, the experimental setup was studied by comparing the solutions adopted with the guidelines given in ASTM-E756-05. An exhaustive validation of the values obtained is then reported.

## 1. Introduction

Noise and vibration control is a relevant design requirement in several industries, such as aerospace and automotive, being the reduction of these two phenomena a major criterion for achieving customer satisfaction [1][2][3]. Passive damping technology often uses viscoelastic materials to decrease the vibratory level transmitted and noise field generated. Because of the peculiar properties of these materials, the mechanical energy is transformed into heat and subsequently dissipated. Used since the 1950s, traditional treatments envisage the deposition of a ply of damping material on the interested surface (free layer damping, or FLD). The main concept of this intervention is that the shear strain acting in the viscoelastic layer stores some energy that is drained from vibrations. Improvements in damping have been achieved with the introduction of a conveniently designed constraining lamina at the free surface (constrained layer damping, or CLD). This configuration results in higher performances with relatively small penalties in weight. There is an extensive body of literature on methods suitable for predicting the intrinsic properties of beams and panels treated in these ways, and the results of their use in fundamental studies and actual applications have been published since the end of the 1950s [4]-[10]. An exhaustive survey of these prediction methods is presented in [11]. Several applications of viscoelastic damping for noise control in the automotive and aircraft fields are presented in [12]. More recent papers approach the same problem using the Finite Element (FE) method [13][14][15].

In terms of actual applications, the constrained layers are mainly observed as an a posteriori intervention needed to fulfil noise requirements not satisfied by the bare structure. Even if these methodologies can generate suboptimal solutions in terms of vibration-performance-over-weight ratios, the separation between dissipative and structural functions has the advantage of not affecting the standard design process. Either analytical or finite element methods can be used to satisfy structural integrity requirements, and the presence of dissipative treatments can be neglected when discussing such requirements.

The growing use of such dissipation mechanisms has motivated many authors to study a deeper integration of viscoelastic layers (integrated layer damping, or ILD) into the structural panel at the expense of simplicity. The concept of damped structures composed of metal-viscoelastic or composite-viscoelastic sandwiches allows for an improvement in the vibro-acoustic behaviour even if the drawbacks in terms of structural efficiency are still not obvious [16] [17] [36].

Regardless of the treatment type (free, constrained or interleaved layer damping) and the predictive method employed (e.g., Ross-Kerwin-Ungar formulation, modal strain energy, frequency response derived from finite element model), reliable information about the constitutive laws of the viscoelastic material must be acquired. This requirement is typically satisfied by measuring the complex modulus, namely, the frequency behaviour of the shear modulus  $G(f)$  and loss factor  $\eta(f)$ .

This task is often taken for granted in many works, e.g., [18] and [19]. However, this task actually represents a challenge from an operative perspective because of the large number of factors that influence the characteristics of rubbers, e.g., temperature, strain level, speed of load application, and pre-stress state. In [20], the presence of nonlinear effects is outlined and confirmed based on experimental observations. In [21], the Golla–Hughes method is applied to develop a finite element model suitable for identifying a model in the time domain with application to a low-frequency range. In [23], an experimental setup suitable for dynamic tests is presented. However, problems are generally magnified at the high frequencies typically involved in noise applications; the setup and operation of such experimental rigs tend to become more difficult as the upper frequency bound increases.

The properties of a VEM can also be characterised directly in a relatively low frequency range. The temperature-frequency equivalence is then employed to project data into a higher frequency range. However, this approach, based on the classical theory for Dynamic Mechanical Thermal Analysis (DMTA), is not of general validity, e.g., it is not applicable in the case of blended materials [22].

In the present study, the properties of a Styrene Butadiene Rubber were evaluated at relatively high frequencies of up to 2,500 Hz, which cover typical helicopter applications.

The cantilever beam method, typically based on the Oberst method [24], was used but linked to other techniques to overcome the previously mentioned theoretical limitations of the DMTA approach; this approach has also been used by other researchers, e.g., [13]. The ASTM E756-05 document [25] describes a number of guidelines for the reliable experimental characterisation of viscoelastic materials. One guideline suggests size ratios of a metal/viscoelastic/metal sandwich specimen: for a typical specimen the length should be approximately 250 mm, the width approximately 10 mm and the metal layer thickness approximately 10 times that of the viscoelastic one, approximately a few millimetres. With these dimensions, the presence of few bending modes suitable for experimental identification below 3,000 Hz can be easily verified, as later discussed in Sec. 3. This fact could make it difficult to obtain a reliable frequency-dependent regressive model in the band of interest. Furthermore, the advised thickness ratio could vary considerably for typical applications, thus possibly introducing discrepancies

in the actual strain level acting in the dissipative ply as well as nonlinear effects. In contrast, the use of thinner metallic layers makes the experiment prone to other effects, namely, mode shapes different from bending, the coupling of bending deflection with twists, modes straining the cross section in the transversal direction and modes with longitudinal bending waves. In these cases, the data processing conceived assuming a pure bending deflection cannot be easily applied. The path presented in other studies based on a mixed approach, e.g., [26], was retraced by using correlation techniques to identify the shear modulus but working only with experimentally identified modal data reliably correlated to finite element models. Furthermore, the Modal Strain Energy approach, based on finite element models, is used to determine the material loss factor. A free-specimen geometry was assumed to allow for the use of metal/viscoelastic/metal sandwich size ratios close to the application at hand, and the effects of the eigenvector shapes were accounted for by utilising a finite element model and a correlation procedure widely used in experimental modal analysis. A section of the paper is devoted to the presentation and discussion of results and issues concerning such procedures. Two of the specimens available from a previous study were used to perform the identification procedure. Additional test data related to other layouts were used to confirm the correctness and reliability of the identified data under different conditions.

## 2. Method for estimating properties of a viscoelastic material

Viscoelastic materials exhibit a combination of viscous and elastic behaviours, with the relative contributions being dependent mainly on the temperature and frequency, or strain rate. This effect introduces a delay between the input strain and output stress at a given frequency. A simplified frequency modellisation is often assumed to account for such a delay: the frequency description of the viscoelastic behaviour is based on the elastic/viscoelastic equivalence principle. It is also possible to formulate viscoelasticity problems in the framework of elasticity theory with complex Young's and shear moduli depending on the frequency [1][2][3]. Because viscoelastic materials are mainly used in shear strain conditions, the relevant stress-strain law suitable to characterise the hysteretic damping can be reduced to the complex shear modulus  $G^*(f)$ . The storage and shear loss moduli  $G'$  and  $G''$ , respectively, are introduced in terms of real and imaginary parts as follows:

$$G^*(f) = G'(f) + iG''(f) = G'(f)[1 + i\eta(f)] \quad (1)$$

The relation between the shear loss factor and modal damping is useful for identifying this modellisation with the modal experimental results:

$$2 \cdot \zeta(f) = \eta(f) = \frac{G''(f)}{G'(f)} \quad (2)$$

However, a fully three-dimensional stress-strain law can be developed by simply assuming the Poisson's ratio not frequency dependent [28]. An inverse procedure can be adopted to establish the viscoelastic properties assuming that a suitable set of pairs resonance frequency-loss factors are available from the experimental data for hybrid specimens related to metal/rubber stacking.

### 2.1 Estimation of the shear modulus

Two methods are available for determining  $G'(f)$ . The first method, which is purely analytical, is based on the theory of De Saint Venant and is described in [25]. The main advantage of this simplified

technique is the short time needed to obtain the curve; however, this technique also has several potential drawbacks, such as the requirement to use only bending modes to define the frequency behaviour or the hypothesis that layers remain straight along the width, a questionable assumption at high frequencies.

The second method is based on the identification of mechanical properties using a classical correlation process; a real eigenvalue analysis of a detailed finite element model linked to an optimisation process to match experimental data: assuming known data for the constraint layer materials, the shear modulus of the dissipative material is modified until the frequency of the desired mode matches the experimental value.

The last technique was deemed more suitable for this work despite its longer time requirement because it guarantees a deeper insight into the dynamic behaviour of the specimen. The elastic property ( $E$ ) of the viscoelastic material is identified at the modal frequencies by matching the measured frequency with the corresponding finite element frequencies.

The value of  $G'$  is updated based on the formula

$$G'(f) = \frac{1}{2(1+\nu)} E'(f) \quad (3)$$

The tuning was realised by iteratively setting the viscoelastic elastic properties to match a single mode frequency at once. Thus, a frequency-dependent law for both the Young's and shear moduli is obtained. The matched displacement modes are saved together with the derived data (frequency and modal strain energies, total and fractional in the viscoelastic layer) for the following viscoelastic loss factor estimation.

The analysis used to calculate the modes is a real eigenvalue extraction. The experimental resonance frequencies depend on damping, although this influence is neglected in the finite element model. To consider this effect, an a posteriori correction of the calculated values is performed based on the behaviour of a single damped degree of freedom using the well-known formula

$$f_{updated} = f_{FEM} \cdot \sqrt{1 - \zeta^2} \quad (4)$$

A fitting curve is then derived to interpolate the frequency dependence of the viscoelastic material moduli.

## 2.2 Estimation of the loss factor

There are several methods for metal-rubber-metal sandwich panel loss factor estimation, and these methods can be divided into two classes. The first class supplies the estimation without considering the geometrical shape of the object (e.g., shape and boundary conditions), and it is trimmed based solely on the bending behaviour. The second class is suitable for predicting the behaviour of a specific structural element manufactured with the hybrid technology without the limit concerning the mode type, and it is generally based on a finite element formulation of the problem.

The methods referring to the first category are as follows:

- The Ross-Kerwin-Ungar approach, which, in its standard formulation, is usable only with a single viscoelastic inclusion;
- The General Laminate model [27], implemented in the ESI VAOne code [29] to predict subsystems properties in the frame of a Statistical Energy Analysis, namely the damping in linear viscoelastic laminates, thanks to a wave propagation analysis. It can be used for any type of stacking sequence and number of viscoelastic inclusions.

Methods devoted to the prediction of the behaviour of specific structural elements are as follows:

- The finite element Direct Frequency Response [30];
- The Modal Strain Energy method [31].

All of the previous methods have worthwhile benefits but also some limitations. To obtain the loss factor frequency behaviour of the viscoelastic, the use of a predictive method for damping in hybrid laminate is needed. In this work the modal strain energy method is envisaged but in a reversed manner. This method, which is a compelling option in terms of flexibility, reliability and time consumption, was applied in its basic implementation [31] even though improvements are available in the literature, e.g., [32]. This method is based on the real eigenvalue analysis of a finite element model from which one can derive the total Strain Energy,  $SE_{Total}$ , as well its amount stored in the viscoelastic core,  $SE_{Visc}$ , and into the constrain layers,  $SE_{Cons}$ . These data are available for each mode,  $SE(f)$ , thus allowing for the development of a frequency law. Based on this approach, the global loss factor of the model can be stated as a sum of individual material loss factors, each weighted with the corresponding fraction of modal strain energy:

$$\zeta_{Test}(f) = \frac{\zeta_{Visc}(f)SE_{Visc}(f) + \zeta_{Cons}(f)SE_{Cons}(f)}{SE_{Total}(f)} = \zeta_{Visc}(f)FSE_{Visc}(f) + \zeta_{Cons}(f)FSE_{Cons}(f) \quad (5)$$

In Eq. (5), the Fractional Strain Energy (FSE) has been introduced for the viscoelastic and the constraint layers. An available structural loss factor can be projected on the unknown viscoelastic material for each specific mode, and thus, a frequency shaping can be obtained as follows:

$$\zeta_{Visc}(f_i) = \frac{1}{FSE_{Visc}(f_i)} \zeta_{Test}(f_i) - \frac{FSE_{Cons}(f_i)}{FSE_{Visc}(f_i)} \zeta_{Cons}(f_i) \quad (6)$$

Assuming that the aluminium alloy provides a negligible contribution, which holds for most structural materials, the equations can be simplified to

$$\zeta_{Visc}(f) = \frac{1}{FSE_{Visc}(f)} \zeta_{Test}(f). \quad (7)$$

Finally, by assuming the availability of the specimen loss factor behaviour, e.g., from experimental data, and results from finite element analyses (the frequency and strain energy saved during the shear modulus estimation step described in the previous section), Eq.(7) can be applied to the modes in the entire frequency range of interest to define the loss factor frequency behaviour.

### 3. Experimental guidelines from finite element models

The availability of finite element models allows computations to be performed to support the experimental activity. Qualitative information concerning the specimen dimensions, sensor positioning, mode shapes and modal density in the investigated frequency band can be obtained by using a plausible trend of the storage modulus  $G'$  and loss factor  $\eta$  curves for the viscoelastic material.

Being the proposed approach based on the reversed use of the modal strain energy method, the sensitivity of this indicator with respect to the experimental setup, i.e., specimen sizes, constraints or inputs, must be discussed.

The effects due to the specimen sizes were first investigated. The ASTM rule is not strictly mandatory for such items, but the free length is suggested to range between 180 and 250 mm, and the width should

be approximately 10 mm. A constraining metallic layer thickness of approximately ten times the thickness of the rubber layer is also suggested. Once these suggestions have been incorporated, a 225 mm x 10 mm specimen with a 0.38-mm-thick viscoelastic layer (the nominal thickness of the Styrene-Butadiene-Rubber used in [17]) and 4-mm-thick constraining layers was numerically tested.

For the case of ideal clamping at one end, tests using this sample would lead to five bending modes within the range of 0-4,000 Hz; once the first mode is excluded, according to the standard, only four points are available to identify the material (triangles in the upper chart of Figure 1). Using the finite element analysis results, it is possible to appreciate that the viscoelastic material stores approximately 30% of the total MSE of the second bending mode, whereas the upper modes indicate a rapidly decaying of this percentage (10% for the fifth mode). Such a small number of points, together with the sensitivity of the MSE inverse procedure to test errors, suggests possible critical issues in the experimental identification. The number of modes in the frequency range as well as the strain energy ratio can be increased by using thinner constraining layers, as shown in the upper chart of Figure 1 by the rhombs, squares and circles related to 2, 1 and 0.5 mm constraint layers thicknesses. Data for torsional modes are presented in the lower chart; in this case, the modal strain energy ratio is rather constant with frequency and progressively increases as the thickness of the constraining layers decreases.

These results suggest that the use of a constraining layer that is thinner than that suggested by the ASTM should be used more effectively to make the modal strain energy method less sensitive to experimental uncertainties; this would also allow a more satisfactorily fitting of the frequency range.

Furthermore, by using a more complex measurement setup than recommended, i.e., one that is also able to detect torsional modes, it is possible to relax the prescription on the width, which is mainly associated with the need to avoid the presence of torsional vibrations within the interested frequency range. The use of a larger specimen (27 and 55 mm wide) with the same boundary conditions and layer thickness ratio led to the data compared in Figure 2 to the narrow, thin specimen. Compared to the 10-mm-wide specimen, the 27-mm-wide specimen exhibits, a similar and regular modal strain energy ratio of bending mode behaviours; the largest specimen (55 mm wide) exhibits the same general pattern but with a non-negligible scattering due to the presence of modes with significant cross-sectional deformation, e.g., longitudinal and high-order bending along the width. The torsional modes of the 27-mm-wide specimen display values approximately three times larger those of the 10-mm-wide specimen and comparable to those for the 55 mm specimen, whose bending and torsional values of modal strain energy overlap considerably. In terms of the number of points available to fit the 0-4,000 Hz range, it would be possible to use up to 18, 24, and 40 points for the 10-, 27-, and 55-mm-wide specimens respectively, compared to the four points available with the basic rule. The availability of a higher number of modes is beneficial because it allows a better fit of the shear modulus and loss factor curves.

In addition, the frequency behaviour of the strain modal energy deserves a discussion. In Figure 3 the strain energies for a typical specimen, total and stored into the rubber layer, are presented with respect to frequencies for all modes, except in-plane ones. Although the total energy frequency dependence exhibits a quadratic behaviour, the energy stored in the viscoelastics increases more slowly, with an approximately linear trend. This holds regardless of the mode type (pure bending and torsion, low and high order, simple and complex pattern). The constant decrease in the fractional strain energy with increasing frequency is common to all of the laminations discussed in the next section, and the net effect is to emphasise the difficulties for a reliable loss factor identification at high frequencies. At high frequencies, the identification algorithms exhibit a larger uncertainty, especially in the case of highly

damped structures. Furthermore, errors in the laminate modal damping measurements are amplified, and the ratio of  $SE_{Total}$  to  $SE_{Visc}$  in Eq. 7 is large. Thus, the identification of the damping properties in the upper frequency range may be not sufficiently accurate. Furthermore, the simplification of Eq. 6 to Eq. 7 may no longer be valid when high values of the  $\frac{FSE_{Cons}}{FSE_{Visc}}$  ratio make the second terms in Eq. 6 relevant with respect to the first one, despite usual negligible values of  $\zeta_{Cons}$ .

From a conceptual point of view two independent sets of experimental and finite element modes must be matched to use Eq. 7. Errors in the mode pair table compilation impact the loss factor determination, especially when bending and torsional modes have different total-to-viscoelastic strain energy ratios.

The modes are easily identified when using the narrow and thick specimens and the measurement setup suggested by ASTM E756-05; specifically, the modes are well spaced in frequency, spacing is increasing with frequency and the progression in terms of waves is regular and easily predictable. In contrast, the presence of modes with complex shapes must be accounted for when using thinner and larger specimens, due to the presence of higher-order modes, particularly with transversal waves, at relatively low frequencies. To correctly link these eigenvectors, spatial aliasing problems should be avoided, i.e., using three or more sensors along the width of the specimen; however this would entail an excessive increase in the setup complexity and costs.

Related to the previous discussion is also the fact that laminations, characterised by higher fractions of viscoelastic strain energy, tend to diminish the effects of experimental uncertainty. This result can be achieved using either a multilayer configuration or a single-layer configuration with a large thickness for the dissipative material. These methods both have some limitations: the first one requires a more difficult technology, and the thermal cycle used to vulcanise the viscoelastic material may be unable to produce rubber layers with identical thicknesses and mechanical properties. The main limitation of the second configuration is related to the low stiffness of the specimen, which prevents high frequencies from being attained.

Thus, rather than complicating the experimental setup, the approach adopted in this study is based on three actions: 1) to make available a large number of modes using thinner and larger specimens, 2) to identify modes with a relatively coarse measurement grid and 3) to discard mode pairs with poor matching qualities. This latter validation is performed by means of the Modal Assurance Criterion applied among experimental and numerical modes (Cross-MAC analysis) [37]. This technique, based on the evaluation of the parallelism of two vectors by normalized scalar product, gives an assessment of the matching between two modes in a scale from 0 to 1, whereas the greater value means a complete correspondence.

This choice leads to a deeper insight regarding the dynamic behaviour of the specimen and to an analytically driven identification procedure that can be summarised in the following steps:

- manufacturing of relatively wide specimens with relatively low thickness ratios or ratios similar to target applications;
- use of typical procedures for multi-point experimental modal analysis (i.e., multiple output locations and a single input location);
- use of correlation techniques between the experimental data and finite element output to identify experimental/analytical mode pairs and reject doubtful cases;

- identification of material properties performed via the modal strain energy method applied to validated modes pairs and experimental loss factors.

Two strategies can be adopted to explore the frequency range of interest: shorten the specimen length, as done in [17], or increase the thickness of the constraining layers. The first technique requires a considerable reduction in the free length to obtain the required increase in modal frequencies with a reduction also in the number of modes available; furthermore it is highly sensitive to the errors in measurement point collocation. Thus, the second method was considered preferable for this study despite the need for two test articles.

Specimens with 0.5- and 1.0-mm-thick constraint layers (AISI 2024 aluminium alloy) and a single viscoelastic inclusion were manufactured as shown in Table 1. They are rectangular and flat (300-mm-long and 50-mm-wide); with the specimen #1 frequencies of up to 1,200 Hz were attained while the range has been extended to 2,500 Hz by means of the specimen #2.

#### **4. Description of the experimental activity and finite element correlation**

The experimental modal analysis was conducted on the specimens, which were clamped at one end between two metallic blocks (overall mass  $\approx 1.0$  kg) so that the free vibration length was approximately 225 mm. The seismic mass is suspended via elastic cables to react to rigid motions and forced to input disturbances into the specimen. A nylon stinger was used to provide excitation, and a PCB 208C01 load cell was adopted to measure this excitation. The load cell was linked to the block far from the mid axes of the specimen to supply an adequate input for the torsional modes. Compared to a classical free-free suspension, this setup allows us to host the load cell and to transmit the force without any unwanted addition of either mass or stiffness to the specimen. Thus, the vibration test is similar to a shaker table [33] but different from a standard modal experiment, in which the structure being tested is directly excited. The response was measured by a low-mass accelerometer (PCB™ 352C22, mass 0.5 g), moved to each position of a mesh of fourteen measurement, regularly arranged in two columns, of seven rows each points. The points allow to recover up to fifth-order mode shapes, for both bending and torsional modes. A special cable from PCB was used to reduce the invasiveness of the wiring. The setup is detailed in Figure 4.

The temperature was monitored but not controlled: during the tests, it ranged from 18°C to 22°C, and such changes were considered sufficiently small to be neglected.

An excitation by an electro-mechanical shaker has been preferred to impulsive tests with instrumented hammer due to the problems of repeatability and limited band. A swept sine input was used instead a random one to ensure a greater degree of control of the load amplitude across the whole frequency range. A sensitivity study of this parameter was deferred to future studies. A linearly swept sine from 5 Hz to 4 kHz was used with an amplitude profile that increases with frequency. Frequency rates of 1 and 10 Hz/s were chosen for the lower and upper parts of the band, respectively. The lower value at the low frequencies was chosen to allow sufficient time for the vibration to develop more cycles. No control strategy was used for the force produced by the shaker. Repetitions of the acquisition were performed during the test, mainly for monitoring and quality purposes, but not in a systematic manner because of: the good repeatability, high cleanness of the frequency response functions and the high signal to noise ratio observed. The Polimax algorithm [34], from TestLab by LMS-Siemens, was used for modal identification.

The finite element models were prepared and analysed by MSC/NASTRAN. They are based on a full solid modellization with 8-node solid linear elements (CHEXA8), about 2mm long and wide, while a single element was used in the thickness direction for each layer: the mesh in this case was made of 113x28x3 elements. This discretization was the result of a convergence analysis carried out with respect to in plane element sizes (length and width) on a ideally clamped specimen: analysis with sides of elements of 5, 4, 3 and 2mm were performed. The deviations in eigenfrequencies of the first 20 modes have been considered, stopping the refinement with deviations below 0.5%; the adopted discretization led to about 20 elements in the shortest bending mode wavelength. A further convergence check was then carried out on the strain energy values by halving the in plane element size and using four elements along the thickness direction for each layers: among 27 modes in the frequency range 0-2500Hz two of them showed discrepancies in fractional strain energy values about 1%, only the first in-plane mode was above such limit (5%), while data for the other modes were well below 1%. Figure 5 provides an example of the finite element models in terms of overall view and details.

The elastic properties of the AISI 2024-T3 aluminium alloy used for the two external laminae were determined based on Aerospace Specification Material (ASM) datasheets (Young modulus 73.1 GPa, Poisson's coefficient 0.33, volume density 2,780 kg/m<sup>3</sup> and negligible damping). To initiate the procedure the information available for the SBR are used, included a density of 1,450 kg/m<sup>3</sup> and, based on previous remarks, a Poisson's coefficient of 0.49; the latter, slightly lower than 0.5, is suitable for approximating the behaviour of such materials while avoiding numerical issues with the solver.

## 5. Identification of the viscoelastic properties

The procedure described in Section 2 was performed to identify the properties of the viscoelastic material. An experimental modal analysis of the two specimens led to the mode frequency and damping results summarised in Figure 6. These results display both bending and torsional modal damping values. For a generic hybrid laminate, modal damping does not lay on a smooth curve but is instead strongly dependent on the type of modal shape. Even if a portion of the data scattering is due to experimental errors, the main portion of the scattering must be ascribed to a different mechanisms of activation for the dissipative phenomenon between the various modes. These differences are mitigated by the Modal Strain Energy method used in the viscoelastic identification procedure.

The properties of the damping layer were then modified in the finite element models to tune the frequencies only for well correlated modal shapes: thanks to the availability of experimental modes, the Modal Assurance Criterion (Cross-MAC) [37] was used so that the effect of experimental uncertainties are reduced. An example of this analysis is provided in Figure 7. Problems in identification of experimental modes can derive from several reasons: low frequency separation between two modes characterized by high damping, sub optimal position of the input force, noise in the responses are only some of the possible causes. During the tests it has been noticed that the eigenvectors of poor quality exhibit even completely erroneous damping values. With a rule of thumb it has been chosen to use only the experimental modes with Cross-MAC coefficients higher than 0.60 to identify the Styrene-Butadiene-Rubber characteristics. This threshold has been identified by experience but it resulted to be a good value to discern between badly and well estimated experimental loss factor: indeed modes with very stable identified properties exhibit cross-MAC values well above 0.8-0.9, while for more doubtfully identified modes they quickly decay even to values below 0.2. Only one mode in the high frequency band would be excluded by a higher threshold. The modal frequencies and damping of correlated modes

satisfying such criteria are presented in Table 2. About ten modes satisfy the correlation requirements for each specimen, with values that in the most cases pass 0.9. The modal strain energy method was used in a reversed form to determine the dissipative behaviour of the specimens. The data and results are summarised in Tables 3 and 4, where the following results are listed:

- Experimentally identified frequencies (measured and corrected) and loss factors,
- Finite element mode frequencies and Young's modulus (after the  $G'$  assessment procedure),
- Fractional Strain Energy in the viscoelastic material (based on Eq. 5),
- Fractional Strain Energy ratios (as defined in Eq. 6),
- Loss factor of rubber (obtained from Eq. 7).

Based on the fractional strain energy ratios of the modes under consideration and on a structural loss factor of  $1.0 \times 10^{-4}$  for the aluminium alloy [3], Eq. 6 can be reduced to Eq. 7 for differences below 0.2% in the loss factor; however, for the first modes, this difference is approximately 0.5%.

The shear modulus data with respect to frequency produced by the procedure are presented in Figure 8. These data can be used to appreciate the of scatter of the results obtained from two different specimens. A logarithmic fitting curve, according to [22], of the entire dataset was calculated, and its equation is assumed to be valid in the range of 100-2,500 Hz:

$$E(f) = 6.3847 \cdot \ln(f) - 16.565 \text{ MPa} \quad (8)$$

Based on the previous cited relation between  $E$  and  $G'$ , Eq. (8) leads to

$$G'(f) = 2.1282 \cdot \ln(f) - 5.5217 \text{ MPa} \quad (9)$$

The second part of the procedure was performed to identify the damping properties in terms of the loss factor. For each mode, the fractional strain energy was recovered and used to determinate the frequency trend of the SBR loss factor according to Eq. 7. Figure 9 presents the estimated damping data: the data scattering increases with increasing frequency; however, the curve trend is still clearly visible.

A curve fitting of the entire dataset is obtained, again in logarithmic form, and is assumed to be valid in the range of 100-2,500 Hz:

$$\zeta(f) = 1.8487 \cdot \ln(f) - 5.1500 \% \quad (10)$$

## 6. Validation of the identified viscoelastic material model

The first step in validating the damping curve of viscoelastic material was to analyse the dissipative behaviour of the two specimens used during the characterisation. The direct modal strain energy method was used with the data presented in Tables 3 and 4. The  $G'$  fitting curve is not influential in this comparison. The correlation between the two datasets is presented in Figure 10 in terms of the damping values for bending and torsional modes obtained by measurements and by the prediction model. The thin specimen produces data with a lower scattering than the thicker specimen.

To further validate the complex modulus obtained, the data presented in [17] are compared with the predictions obtained from modal strain energy strategy fed with present correlated viscoelastic properties. In that study specimens were manufactured with several laminations and materials (metallic and composite), all made with inclusions of the same dissipative material studied in this paper. Only data related to specimens batches made of aluminium alloy have been considered for the comparison in the present work. The set was completed with the manufacturing and testing of a thick specimen, with a

thickness ratio based on ASTM suggestions (batch #18 with 4mm constraint layers). Only bending modes were measured in [17], and thus, the comparison is limited to these modes. Specimen data are summarized in Table 5. The predictions are compared in terms of the loss factor of various stacking sequences so that the degree of likeness of the prediction is made for specimens whose experimental data are not involved in the characterisation procedure.

To estimate the damping using a modal strain energy approach, an iterative procedure should be needed to calculate the modal strain energy at a given frequency with a correct value of  $G'$ . Because this method is time consuming, an alternative approach was preferred. The modified Modal Strain Energy method allows the loss factor to be projected over the entire desired frequency range in a simple manner. It does not consider the change in the storage modulus during the finite element analysis but incorporates its effect into the results a posteriori [31]. The shear modulus of the viscoelastic material is kept constant to a reference value in the modal analysis, thus allowing a single real eigenvalue analysis, while the effect of its frequency variations is accounted for by scaling the strain energy of the viscoelastic material by the square root of the shear modulus at the frequency of the mode under consideration normalized with respect to a reference value as follows:

$$\zeta_{Global}(f) = \zeta_{Visc}(f) \frac{SE_{Visc}(f)}{SE_{Total}(f)} \sqrt{\frac{G'(f)}{G'_{Ref}}} \quad (11)$$

This method simplifies the relationship between the shear modulus and frequency; however, the method is often used to forecast the behaviour of hybrid laminate objects due to its simplicity. A  $G'$  of 6.66 MPa was chosen as a reference. How this choice affects the results is beyond the scope of this article and deferred to future studies.

The specimens can be divided into two sets, the first referring to a single viscoelastic inclusion, that is, the classic metal/polymer/metal sandwich, and the second one referring to multiple staking sequences. The results for the first set (i.e., Batches 6 to 8) with increasing viscoelastic layer thickness are reported in Figure 11-Figure 13. The simplified finite element approach matches the experimental results quite well for the three specimens even though the shear modulus is slightly underestimated at frequencies below 250 Hz whilst overestimated at frequencies between 500 and 1,700 Hz. These differences are likely due to the simplification of the dependence of  $G'$  on the frequency. These effects will be investigated in future work. For completeness, a comparison with two alternative models is presented (the classic RKU formulation and the General Laminate model). All predictions are similar with a consistent overestimation of damping above 500 Hz.

The comparison of results obtained for the set of samples with multiple viscoelastic inclusions (batches #9-12) is now presented. The samples #9-12 are all based on the same type of structural layers (AISI 2024, 0.5 mm) but with a different number of viscoelastic and metallic inclusions. The experimental data are compared in Figure 14 -Figure 18 to the results from the simulation procedures using modified Modal Strain Energy and General Laminate approaches; the comparison is again related to bending modes. The predicted laminate loss factor is in good agreement with the experimental data.

Finally, the results for batch #18, the thick case (two 4-mm layers of AISI 2024 and a single 0.38-mm viscoelastic inclusion), are presented in Figure 19. In this case, the predictions underestimate the damping in the low-medium frequency range regardless of the method employed.

The identified model of the viscoelastic material allowed the prediction of laminate loss factor very similar to experimental data for specimens that differed considerably, compared to the samples used in the characterisation step, in terms of both stiffness and layout.

## **7. Concluding remarks and future work**

In this study, well-known techniques, for the standard experimental modal analysis and correlation of finite element models with test data, combined with the Modal Strain Energy method have been used to identify the frequency-dependent properties of a viscoelastic material. The procedure, which differs from the ASTM rules, was conceived with the aim of identifying the shear modulus and damping loss factor within a medium-high frequency range of 100-2,500 Hz suitable for vibro-acoustic analyses.

Guidelines for the selection of the specimen geometry were modified to ensure a satisfactory fitting of the interested frequency range and an adequate sensitivity of the modal strain energy method; although the ASTM rules advise the use of thick and narrow specimens, the adoption of relatively thinner constraint layers and wider specimens was found to be appropriate.

The procedure was applied to identify the shear modulus and damping loss factor of a Styrene Butadiene Rubber. Two specimens, with a single viscoelastic layers constrained between two metallic sheets, were used. The specimens were manufactured with different thicknesses to achieve different bending stiffness, thus allowing for a better fitting of the frequency domain.

The use of the Modal Assurance Criterion, to reject unreliable experimental data, allowed for the development of a method that is robust with respect to experimental uncertainties, namely because of the conceptual difficulties in adopting standard identification methods for highly damped specimens.

The reliability of the results obtained was verified through an extensive application of a prediction method, based again on the modal strain energy method but also on alternate implementation, to a set of specimens with very different properties. The laminate loss factor was estimated accurately regardless of the amount of rubber in a single viscoelastic inclusion as well as in cases with multiple viscoelastic inclusions.

A more in-depth investigation of some aspects, important for actual applications, was postponed to future work, including a discussion of the effects of the choice of the reference shear modulus used in Eq. (11).

## **ACKNOWLEDGEMENTS**

The authors would like to thank Alessandro Perazzolo from AgustaWestland for his support with VAOne analyses.

## **8. References**

- [1] F. Fahy, J. Walker; Fundamentals of Noise and Vibration; New York, E&FN Spon, 1998
- [2] A. Thumann and R. K. Miller; Fundamentals of noise control engineering - Atlanta, GA : Fairmont press, 1986
- [3] M. P. Norton and D. G. Karczub ; Fundamentals of noise and vibration analysis for engineers - 2nd ed. – Cambridge, Cambridge university press, 2003.

- [4] Ross, D., Ungar, E., and Kerwin, E., (1959), Damping of Flexural Vibrations by means of Viscoelastic laminate, Structural Damping, ASME, New York
- [5] Di Taranto, R.A.,(1965), Theory of Vibratory Bending of Elastic and Viscoelastic Layered Finite element Beams, ASME J. Appl. Mech., 87, pp 881-886
- [6] Mead, D.J., and Markus, S., (1969), The forced vibration of a Three-Layer damped sandwich beams with arbitrary boundary conditions, J. Sound Vib.,12(1), pp.271-282
- [7] Mead, D.J., (1970), Loss factors and Resonant Frequencies of Encastre Damped Sandwich Beams, J. Sound Vib., 83(3), pp.363-377.
- [8] Mead, D.J.,(1982), A comparison of some Equations for the Flexural Vibrations of Damped Sandwich Beams, J. Sound and Vib., 83(3), pp.366-377.
- [9] Yan, M.J., (1972), Governing Equations for Vibrating Constrained layer Damping Sandwich Plates and Beams, ASME J. Appl. Mech., 39(4), pp.1041-1046
- [10] Rao, D.K., (1978), Frequency and loss factors of Sandwich Beams under various Boundary Conditions, J. Mech. Eng. Sci., 20(5), pp 271-282.
- [11] C.M.A. Vasques, R.A.S. Moreira and J. Dias Rodrigues, Viscoelastic Damping Technologies–Part I: Modeling and Finite Element Implementation, J. of Adv. Research in Mechanical Engineering (Vol.1-2010/Iss.2) pp. 76-95
- [12] M.D. Rao Recent applications of viscoelastic damping for noise control in automobiles and commercial airplanes, Journal of Sound and Vibration 262 (2003) 457–474
- [13] L. Pan , B. Zhang; A new method for the determination of damping in cocured composite laminates with embedded viscoelastic layer; Journal of Sound and Vibration 319 (2009) 822–831
- [14] K. Amichi, N. Atalla; A New 3D Finite Element for Sandwich Beams With a Viscoelastic Core; Journal of Vibration and Acoustics, April 2009, Vol. 131 021010-1/9
- [15] Z. Xie, W.S. Shepard Jr.; Development of a single-layer finite element and a simplified finite element modeling approach for constrained layer damped structures; Finite Elements in Analysis and Design 45(2009) 530—537
- [16] Di Giulio M., Arena G., Paonessa A., “Vibro-Acoustic Behaviour of composite fuselage structures using embedded viscoelastic damping treatments”, (2009) XX AIDAA Congress, Milano, Italy.
- [17] Ghiringhelli G.L., Terraneo M., Vigoni E. “Improvement of Structures Vibroacoustics by Widespread Embodiment of Viscoelastic Materials”, (2013) Aerospace Science and Technology, Vol. 28, N. 1, p. 227-241

- [18] S.W. Kung R. Singh; Vibration Analysis of Beams with Multiple Constrained Layer Damping Patches; *Journal of Sound and Vibration* (1998) 212(5) 781-805
- [19] R.Fana, G.Menga, J.Yangb, C.Heb; Experimental study of the effect of viscoelastic damping materials on noise and vibration reduction within railway vehicles; *Journal of Sound and Vibration* 319 (2009) 58–7
- [20] G.S. Dutta, C.Venkatesan; Analytical and empirical modeling of multilayered elastomeric Isolators from damping experiments, *Journal of Sound and Vibration* 332(2013)6913–6923
- [21] F.S. Barbosa, M.C.R. Farage, A finite element model for sandwich viscoelastic beams: Experimental and numerical assessment, *Journal of Sound and Vibration* 317 (2008) 91–111
- [22] S. H. Zhang, H. L. Chen, A study on the damping characteristics of laminated composites with integral viscoelastic layers, *Composite Structures* 74 (2006) 63–69
- [23] C.M.A. Vasques, R.A.S. Moreira and J. Dias Rodrigues, Viscoelastic Damping Technologies–Part II: Experimental Identification Procedure and Validation, *J. of Adv. Research in Mechanical Engineering* (Vol.1-2010/Iss.2) pp. 96-110
- [24] H. Oberst, K. Frankenfeld, “Uder die Dampfungder Biegeschwingungen dunner Bleche durch festhaftende Belage”, *Acustica*, 2, pp. 181-194, 1952.
- [25] E756-05 “Standard Test Method for Measuring Vibration-Damping Properties of Materials” rule by ASTM International
- [26] Martarelli M., Santolini C., Perazzolo A., Castellini P., “Damping Properties Assesment of very Highly compliant Sandwich materials: are traditional methods really too old?”, (2012) Proceedings of the 30th IMAC, A Conference on Structural Dynamics.
- [27] P. J. Shorter, “Wave propagation and damping in linear viscoelastic laminates”, (2004) *Journal of Acoustic Society Am.*, Vol. 115, No. 5, Pt. 1.
- [28] Lakes.RS. On Poisson’s ratio in linearly viscoelastic solids, *J. Elasticity* 2006; 85(1):45–63.
- [29] “VA One - Reference Manual”, ESI Group , Paris, 2004
- [30] “MSC/NASTRAN-Reference Manual”, The Macneal-Schwendler Corp. Los Angeles, CA, 2004
- [31] Conor D. Johnson and David A. Kienholz, Finite Element Prediction of Damping in Structures with Constrained Viscoelastic Layers (1982) *AIAA J.* Vol. 20, No. 9, 1284-1290.
- [32] Scarpa F. Landi F.P., Rongong J.A., DeWitt L. and Tomlison G; Improving MSE method for viscoelastic damped structures (2002) *Proc. SPIE* 4697, Smart Structures and Materials: Damping and Isolation, 25.

- [33] J.L. Woitowiki, L. Jaouen, R. Panneton “New approach for the measurement of damping properties of materials using the Oberst beam”, *Review of scientific instruments*, Vol. 75, No. 8, August 2004
- [34] “LMS TestLab, LMS International”, a Siemens Business, Leuven, Belgium
- [35] M. Martinez-Agirre, M.J. Elejabarrieta, Characterisation and modelling of viscoelastically damped sandwich structures, *Int. Journal of Mechanical Sciences* 52 (2010) 1225–1233
- [36] F. Amoroso, A. De Fenza, E. Monaco, R. Pecora, L. Lecce, Experimental evaluation of vibro-acoustic behavior of composite fuselage structures realized with embedded viscoelastic damping treatments, *The 18th International Congress on Sound & Vibration (ICSV)*, Rio De Janeiro - Brazil, July 2011
- [37] Ewins, D. J., “*Modal Testing Theory, Practice, and Application*”, 2nd ed., Research Studies Press, Ltd., 2000, pp. 422-424.

Tables

Spec #	Sizes [mm]	Structural Layers #	Viscoelastic Layers #	Layout
1	300 x 50	2 x 0.5 mm	1 x 0.38 mm	
2	300 x 50	2 x 1.0 mm	1 x 0.38 mm	

Table 1: Specimens for validation

Set 1 (0.5 mm)			Set 2 (1.0 mm)		
Freq. (Hz)	Damp. $\zeta$ (%)	Mode	Freq. (Hz)	Damp. $\zeta$ (%)	Mode
27.10	0.48	1 <sup>st</sup> Ben	54.18	0.73	1 <sup>st</sup> Ben
109.36	1.27	2 <sup>nd</sup> Ben	192.38	1.69	2 <sup>nd</sup> Ben
119.22	1.53	1 <sup>st</sup> Tor	=	=	
279.02	1.82	3 <sup>rd</sup> Ben	472.02	2.09	3 <sup>rd</sup> Ben
365.73	2.40	2 <sup>nd</sup> Tor	597.39	2.74	2 <sup>nd</sup> Tor
497.70	2.63	4 <sup>th</sup> Ben	827.31	3.31	4 <sup>th</sup> Ben
604.75	2.64	3 <sup>rd</sup> Tor	995.45	2.40	3 <sup>rd</sup> Tor
741.78	3.33	5 <sup>th</sup> Ben	1247.62	3.59	5 <sup>th</sup> Ben
851.92	3.36	4 <sup>rd</sup> Tor	=	=	
1103.16	3.07	5 <sup>th</sup> Tor	1853.37	2.74	5 <sup>th</sup> Tor
=	=		1742.36	3.58	6 <sup>th</sup> Ben
=	=		2390.03	3.07	6 <sup>th</sup> Tor

Table 2: Correlated modes

F <sub>Exp</sub> [Hz]	$\eta$ Hybrid [%]	F <sub>Exp</sub> Modified [Hz]	F FEM [Hz]	E FEM [MPa]	FSE <sub>Visc</sub> [%]	FSE Ratio	$\eta$ SBR [%]
27.10	0.96	27.10	27.12	5.20	34.1	1.9303	2.81
109.36	2.54	109.35	109.39	12.25	45.6	1.1908	5.56
119.22	3.06	119.20	119.18	15.70	32.8	2.0486	9.33
279.02	3.64	278.97	278.88	15.80	43.2	1.3167	8.43
365.73	4.80	365.62	365.72	21.55	42.9	1.3328	11.20
497.70	5.26	497.53	497.47	20.30	47.5	1.1041	11.07
604.75	5.28	604.54	604.60	22.80	44.4	1.2535	11.90
741.78	6.66	741.37	741.24	21.70	48.5	1.0615	13.73
851.92	6.72	851.44	851.57	24.95	46.0	1.1729	14.60
1103.1	6.14	1102.5	1102.3	25.65	46.3	1.1614	13.27

Table 3: Description of specimen #1

$F_{Exp}$ [Hz]	$\eta$ Hybrid [%]	$F_{Exp}^{Modified}$ [Hz]	F FEM [Hz]	E FEM [MPa]	$FSE^{Visc}$ [%]	FSE Ratio	$\eta$ SBR [%]
54.18	1.46	54.18	54.18	9.10	30.3	2.2978	4.81
192.38	3.38	192.35	192.36	17.50	33.8	1.9597	10.00
472.02	4.18	471.92	471.88	25.15	38.5	1.5960	10.85
597.39	5.48	597.17	597.24	28.50	37.3	1.6836	14.71
827.31	6.62	826.86	826.42	28.65	39.9	1.5086	16.61
995.45	4.80	995.16	995.14	29.95	36.5	1.7428	13.17
1247.6	7.18	1246.8	1246.3	29.65	36.9	1.7093	19.45
1742.4	7.16	1741.2	1741.0	30.40	32.6	2.0642	21.94
1853.4	5.48	1852.7	1852.5	32.25	32.9	2.0376	16.65
2390.0	6.14	2388.9	2388.8	34.40	35.7	1.8031	17.21

Table 4: Description of specimen #2

Batch #	Structural Layer #	Viscoelastic Layer #	Lay-out
6	2 x 0.5 mm	1 x 0.66 mm	
7	2 x 0.5 mm	1 x 0.84 mm	
8	2 x 0.5 mm	1 x 1.34 mm	
15	3 x 0.5 mm	2 x 0.31 mm	
9	4 x 0.5 mm	3 x 0.31 mm	
10	6 x 0.5 mm	5 x 0.32 mm	
11	8 x 0.5 mm	7 x 0.32 mm	
12	10 x 0.5 mm	9 x 0.31 mm	
18	2 x 4.0 mm	1 x 0.38 mm	

Table 5: Specimens for validation

Figures

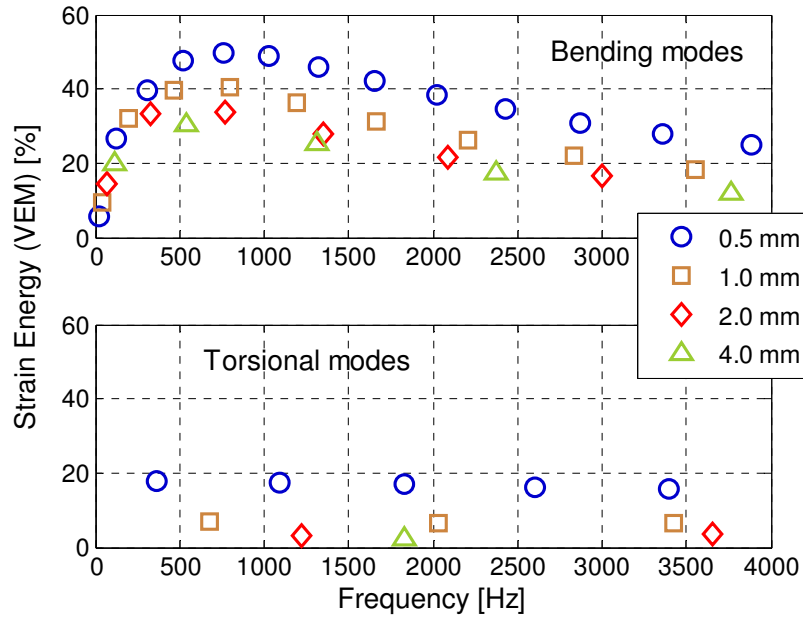


Figure 1: Variation of the strain energy stored in the viscoelastic material as a function of the frequency for different thicknesses of the constraining layers ( 0.5, 1, 2 and 4 mm), for 225 mm long and 10 mm wide beam and 0.3 mm thickness of the viscoelastic layer

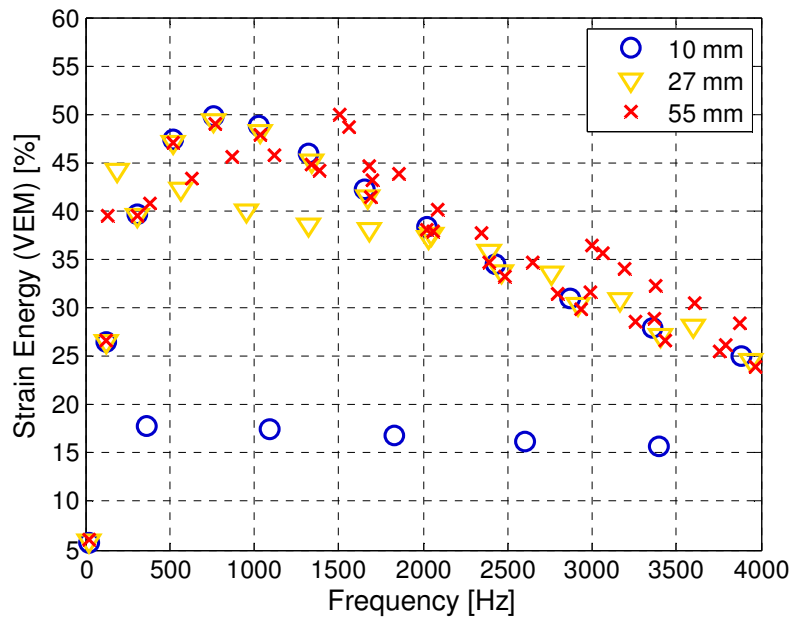


Figure 2: Variation of the strain energy stored in the viscoelastic material as a function of the frequency for different widths of the beams (10, 27 and 55 mm), for 225 mm long beam, 0.5 mm thicknesses of the constraining layers and 0.3 of the viscoelastic layer

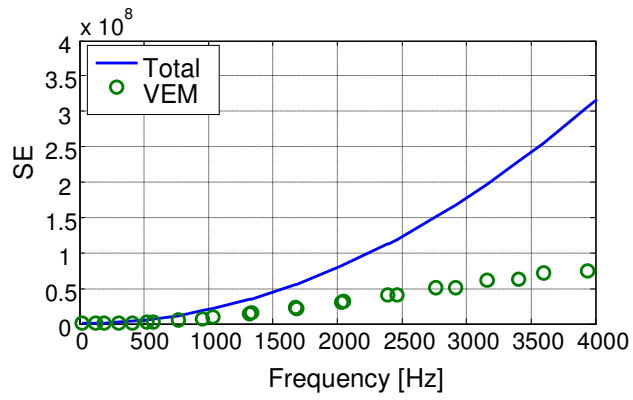


Figure 3: Comparison of the total strain energy and the energy stored in the viscoelastic layer.

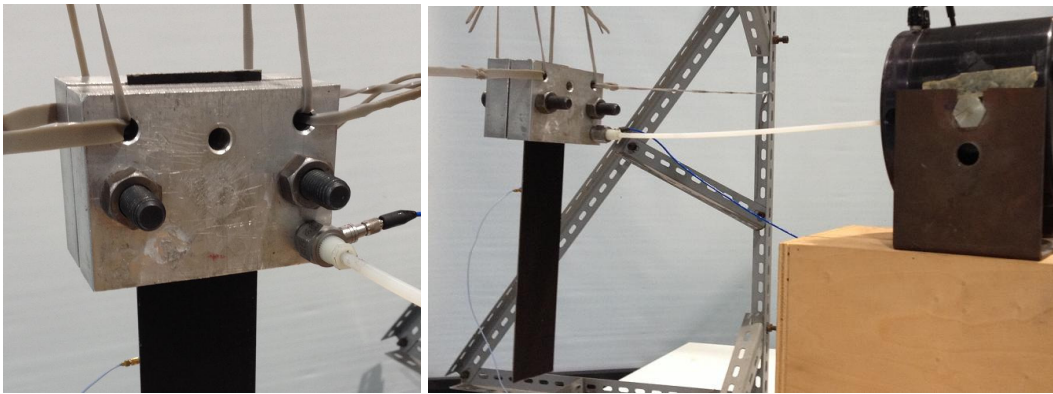


Figure 4: Experimental setup: a) method of excitation and b) overall view.

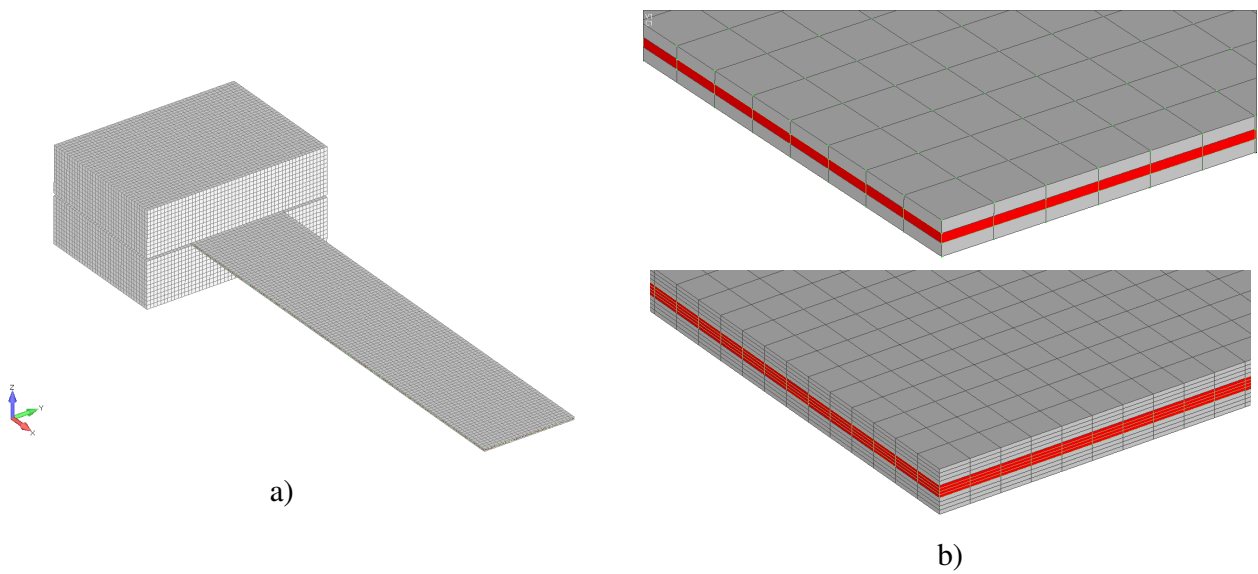


Figure 5: Finite element model: a) overall view and b) details (adopted and refined meshes).

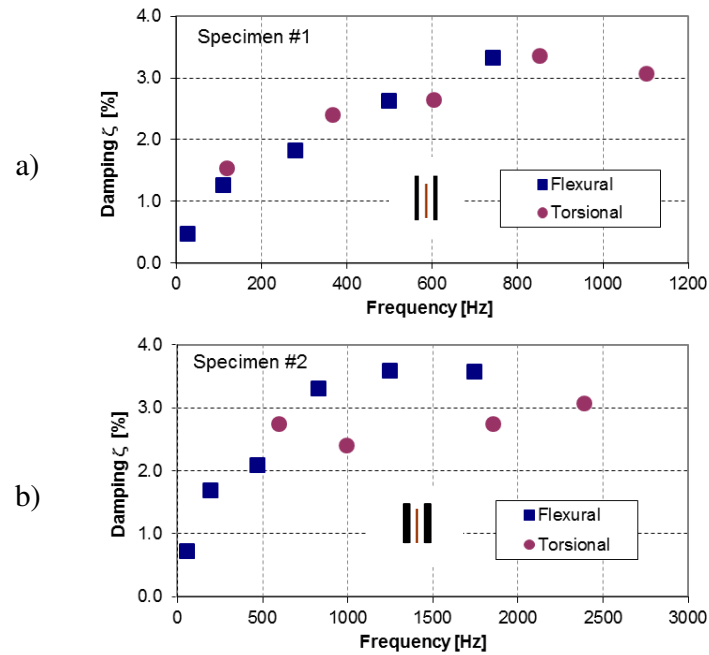


Figure 6: Experimental damping as a function of the frequency derived from a 225 mm long and 50 mm wide beam with a 0.38 thick styrene butadiene rubber interleaved between AISI 2024-T3 aluminium layers: a) two 0.5 mm thick layers and b) two 1.0 mm thick layers.

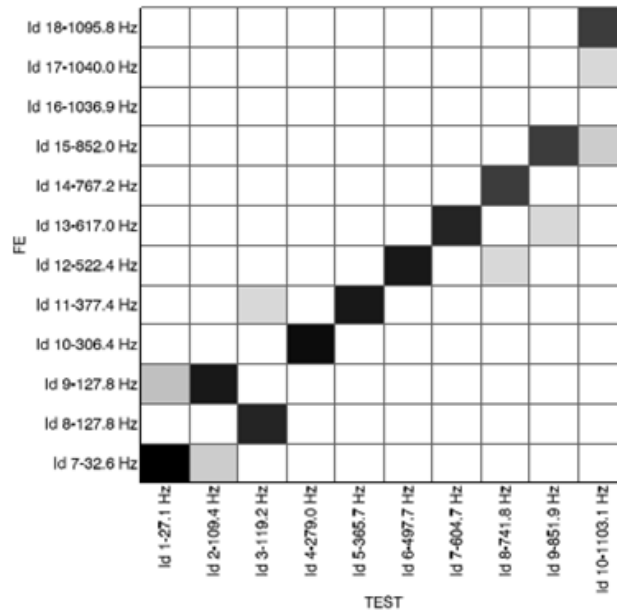


Figure 7: Test/FE CrossMAC (specimen 1)

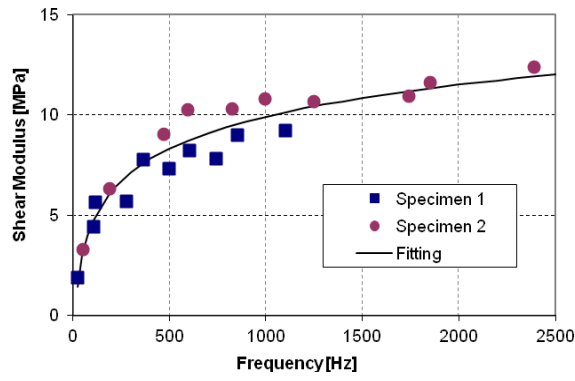


Figure 8: Estimated SBR shear modulus.

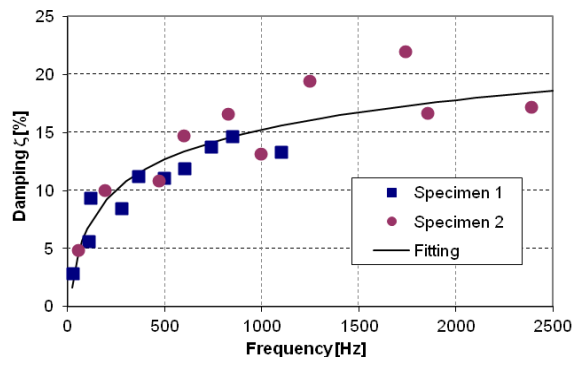


Figure 9: Estimated SBR loss factor.

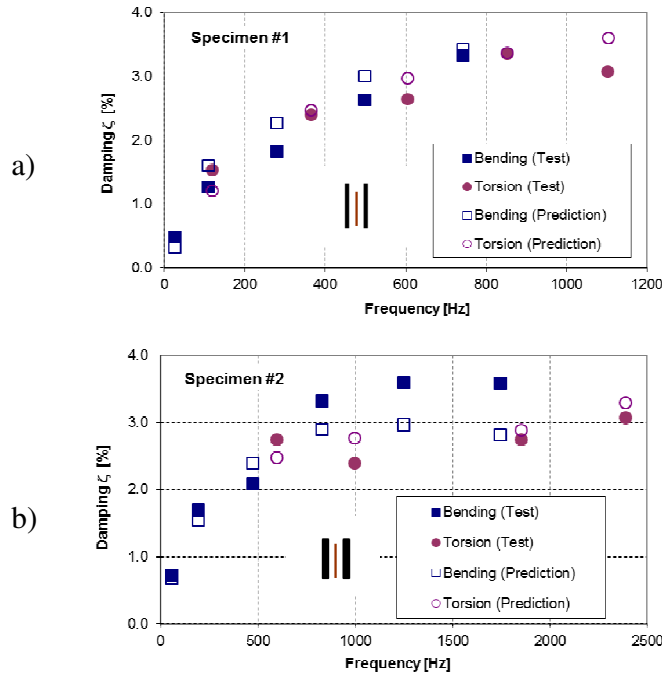


Figure 10: Comparison of the experimental and MSE damping of a) specimen 1 and b) specimen 2.

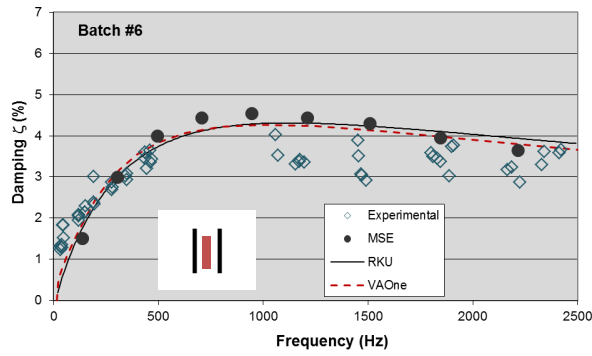


Figure 11: Comparison of the predictions and experimental results for Batch 6.

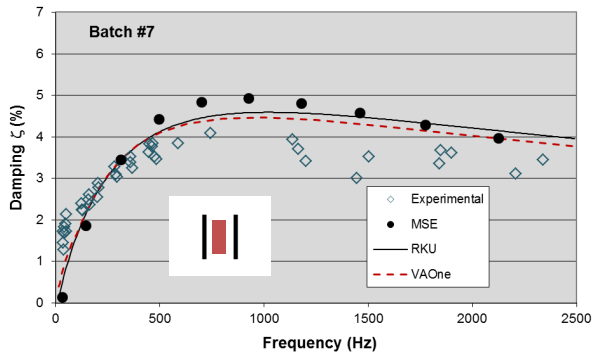


Figure 12: Comparison of the predictions and experimental results for Batch 7.

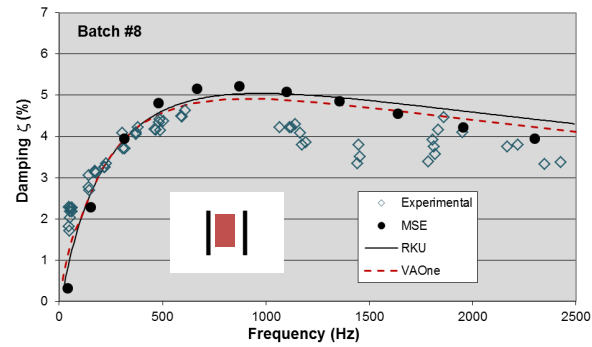


Figure 13: Comparison of the predictions and experimental results for Batch 8.

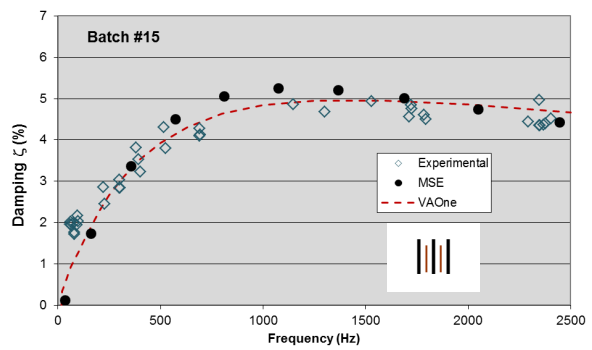


Figure 14: Comparison of the predictions and experimental results for Batch 15.

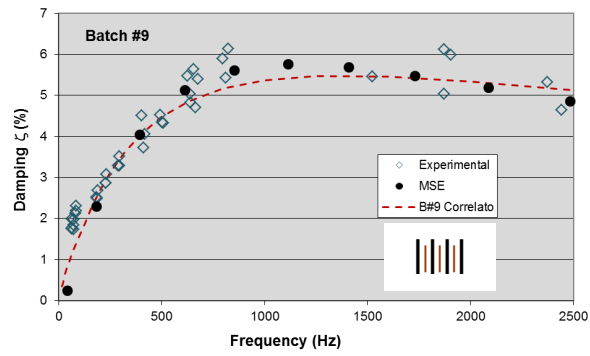


Figure 15: Comparison of the predictions and experimental results for Batch 9.

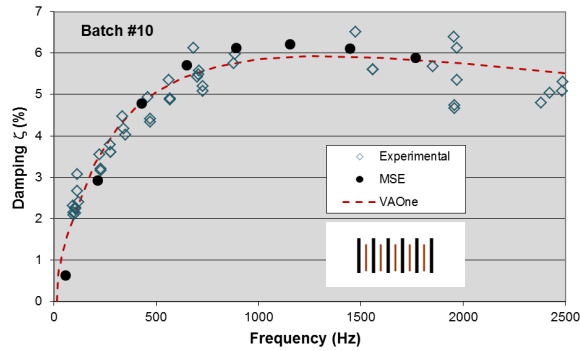


Figure 16: Comparison of the predictions and experimental results for Batch 10.

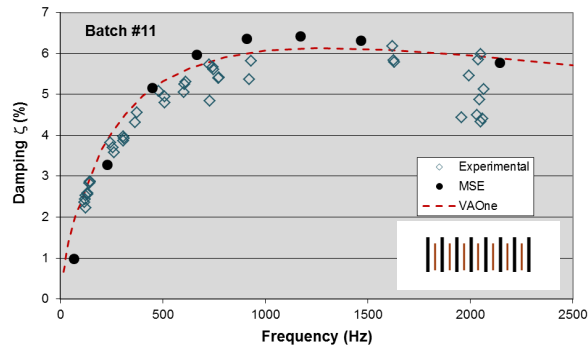


Figure 17: Comparison of the predictions and experimental results for Batch 11.

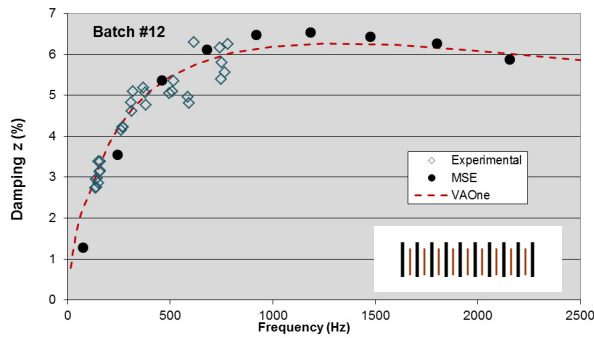


Figure 18: Comparison of the predictions and experimental results for Batch 12.

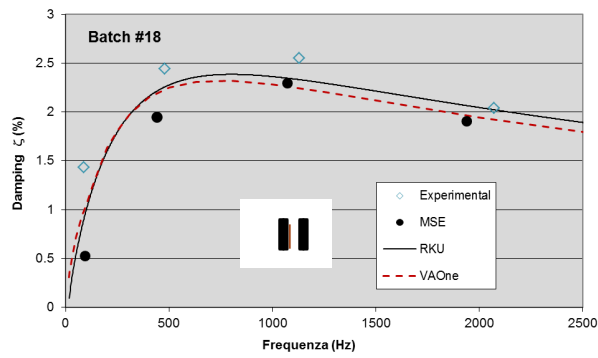


Figure 19: Comparison of the predictions and experimental results for Batch 18.